Unique system of photoreceptors in sea urchin tube feet

Esther M Ullrich-Lüter[a,1], Sam Dupont[b], Enrique Arboleda[c,2], Harald Hausen[d], and Maria Ina Arnone[c,3]

[a]Institut für Evolutionsbiologie and Ökologie, Universität Bonn, 53121 Bonn, Germany; [b]Department of Marine Ecology, The Sven Lovén Centre for Marine Sciences, Gothenburg University, 45034 Fiskebäckskil, Sweden; [c]Cellular and Developmental Biology, Stazione Zoologica Anton Dohrn, 80121 Naples, Italy; and [d]Sars International Centre for Marine Molecular Biology, University of Bergen, 5008 Bergen, Norway

Edited* by Eric H. Davidson, California Institute of Technology, Pasadena, CA, and approved April 4, 2011 (received for review December 10, 2010)

Different sea urchin species show a vast variety of responses to variations in light intensity; however, despite this behavioral evidence for photosensitivity, light sensing in these animals has remained an enigma. Genome information of the recently sequenced purple sea urchin (*Strongylocentrotus purpuratus*) allowed us to address this question from a previously unexplored molecular perspective by localizing expression of the rhabdomeric opsin *Sp-opsin4* and *Sp-pax6*, two genes essential for photoreceptor function and development, respectively. Using a specifically designed antibody against Sp-Opsin4 and in situ hybridization for both genes, we detected expression in two distinct groups of photoreceptor cells (PRCs) located in the animal's numerous tube feet. Specific reactivity of the Sp-Opsin4 antibody with sea star optic cushions, which regulate phototaxis, suggests a similar visual function in sea urchins. Ultrastructural characterization of the sea urchin PRCs revealed them to be of a microvillar receptor type. Our data suggest that echinoderms, in contrast to chordates, deploy a microvillar, r-opsin–expressing PRC type for vision, a feature that has been so far documented only in protostome animals. Surprisingly, sea urchin PRCs lack any associated screening pigment. Indeed, one of the tube foot PRC clusters may account for directional vision by being shaded through the opaque calcite skeleton. The PRC axons connect to the animal internal nervous system, suggesting an integrative function beyond local short circuits. Because juveniles display no phototaxis until skeleton completion, we suggest a model in which the entire sea urchin, deploying its skeleton as PRC screening device, functions as a huge compound eye.

evolution | electron microscopy | immunogold

In most animals, detection of light is a crucial sensory mechanism for interacting with the environment. Sea urchins are no exception and display a huge variety of light-induced behavioral and physiological responses. Reactions upon illumination or shading may (depending on the species) include, for example, color change, spine movements, tube foot reactions, covering, phototaxis, and even spatial vision (1–3).

Contrasting to the wide range of behavioral evidence, no obvious eye-like structure has been reported in sea urchins. Diadematid sea urchins have been mistakenly proposed to possess eyes (4), but later investigators revealed those structures to be iridiophores, which in fact represent the least photosensitive part of diadematid sea urchin skin (2, 5–7). As a consequence, although never proven, sea urchin photosensitivity has been up to now generally assumed to rely on a "diffuse" dermal light sense that uses inconspicuous elements of the superficial epidermal nerve net (2, 3, 8, 9).

The genome sequencing of the purple sea urchin *Strongylocentrotus purpuratus* led to the surprising discovery of a large number of typical "eye" genes, like *pax6*, *atonal*, *neuroD*, and *barh1*, which in vertebrates pattern early retina development (10). Moreover, six different opsins plus other essential components of the signal transduction cascade of photoreceptor cells (PRCs) were identified (10, 11). RT-PCR showed that many of the discovered genes are expressed in adult *S. purpuratus* tube feet (10, 11), suggesting the presence of a more elaborate light-sensing apparatus than was previously assumed.

The aim of this study was to identify the cellular components expressing these molecular players and to unravel a potential mechanism accounting for the complex sea urchin photobehavior. The exploration of an echinoderm photoreceptor system also provided the unique opportunity to bridge a considerable gap in our knowledge of PRC function between protostome and vertebrate animals. In protostomes, microvillar (rhabdomeric) PRCs support vision, whereas in vertebrates this support is facilitated by ciliary PRCs. Until now, the absence of data from deuterostome groups other than vertebrates has made it difficult to unravel the ancestral function of PRC types and to shed light on the evolutionary origin of animal vision. Strikingly, the rhabdomeric type opsin (*Sp-opsin4*) is more strongly expressed than any other opsin type in sea urchin tube feet (10, 11). The use of two key molecular markers, *Sp-opsin4* and *Sp-pax6*, in combination with morphological methods, like transmission electron microscopy (TEM), allowed us to characterize typical microvillar PRCs previously unknown in sea urchins. We found them to be primarily arranged in two clusters in the numerous tube feet and to fulfill the minimal requirements for directional vision by deploying the sea urchin opaque skeleton as a screening device. Taken together, our data support a model of "compound-eye"-like vision in sea urchins contrasting to those proposed for echinoderms by other authors in the past (3, 12, 13). Our findings furthermore constitute unique documentation of a deuterostome animal deploying r-opsin–expressing PRCs for vision.

Results

Evidence for Visual Response in *S. purpuratus*. The accessibility of genomic information, as well as newly available expression data on eye-relevant genes in the sea urchin *S. purpuratus* (10, 11), led us to select this animal as a model for studying echinoderm photoreception. At the start of our investigation, little was known about phototaxis and light-evoked reactions in *S. purpuratus*. We performed behavioral experiments using different artificial light sources (two white light sources and four monochromatic LEDs at 450, 530, 590, and 630 nm) (see *SI Materials and Methods* for details) on adult *S. purpuratus*, and demonstrated that this species shows negative phototaxis upon illumination with maximal reaction at 450 nm (Fig. S1). Similarly to what observed in other echinoderms (1), these sea urchins immediately react to illumi-

Author contributions: E.M.U.-L., H.H., and M.I.A. designed research; E.M.U.-L., S.D., E.A., and M.I.A. performed research; E.M.U.-L., H.H., and M.I.A. analyzed data; and E.M.U.-L., H.H., and M.I.A. wrote the paper.

The authors declare no conflict of interest.

*This Direct Submission article had a prearranged editor.

[1]Present address: Freie Universität Berlin, Institut für Biologie (Zoologie), Königin-Luise-Strasse 1-3, 14195 Berlin, Germany.

[2]Present address: Max F. Perutz Laboratories, Department of Microbiology, Immunobiology, and Genetics, Dr. Bohr-Gasse 9, 1030 Wien, Austria.

[3]To whom correspondence should be addressed. E-mail: miarnone@szn.it.

This article contains supporting information online at www.pnas.org/lookup/suppl/doi:10.1073/pnas.1018495108/-/DCSupplemental.

nation by intensifying tube foot and spine activity and rapidly (at the average speed of 4.6 ± 1.8 cm/min, $n = 20$) move away from the light source to the furthest side of the tank. A reverse reaction is observed when the light source is placed at 180° in the opposite direction. These data confirm preliminary observations of Giese and Farmanfarmaian (14) on *S. purpuratus* scototaxis.

Tube Foot Expression of Visual Genes. We detected expression of two important visual genes, *Sp-opsin4* (a visual pigment clustering with rhabdomeric opsins of other Bilateria) (11) and *Sp-pax6* (the sea urchin *pax6* homolog) (10) in the tube feet of *S. purpuratus* (for tube foot morphology, see Fig. 1*A* and *Inset*). The presence of an opsin clearly indicates light-sensing cells and *pax6* has a conserved upstream position in the gene regulatory network of eye formation in various organisms (15–18). We performed opsin detection at both the mRNA and protein levels using in situ hybridization and a recently developed polyclonal antibody raised against the C terminus of the transmembrane protein, respectively. High specificity of the r-opsin antibody was demonstrated by double-labeling experiments using both antibody and in situ probes (against the mRNA target) of *Sp-opsin4*, showing clear colocalization in single cells (Fig. 1*B* and Fig. S2). According to the long proposed "diffuse" dermal light sense in echinoderms, the photoreceptive tissue would be expected to be found randomly scattered across the neurons of the diffuse nervous system. In contrast to this hypothesis, we found the r-opsin photopigment to be clearly expressed in PRCs in two distinct regions of the sea urchin tube feet (Fig. 1 *C–F*). One array of PRCs is arranged within the rim of the tube foot disk (Fig. 1*D*) and a second cluster resides in a very basal portion of the tube foot stalk where it attaches to the animal's skeleton (Fig.1*E* and Fig. S3). These basal PRCs are embedded in a small cup-shaped groove of the skeleton, where the tube foot nerve enters in the body cavity via a small extra canal accompanying the opening of the tube foot pore (Fig. 1 *G* and *H*). Some more-scattered PRCs also appear along the basal portion of the tube foot nerve, the lateral nerve (Fig. 1*E*), and infrequently within the spine nerves. Each tube foot possesses up to 140 PRCs, resulting in up to 200,000 PRCs per animal, depending on its size and tube foot number.

In agreement with previous findings in *Paracentrotus lividus* (19), strong *pax6* expression was confirmed in the tube foot stalk of adult *S. purpuratus* using in situ-hybridization (Fig. 2*A*). At the base of each tube foot, *pax6* overlaps with the epidermal region expressing the r-opsin protein, although it covers an even larger area (Fig. 2*B*). The situation differs regarding *pax6* expression in the tube foot disk. Here, *pax6* is generally expressed more weakly in regard to the tube foot stalk and in a less-defined pattern. High-resolution double staining of Sp-Opsin4 protein and *pax6* RNA in the tube foot disk did not reveal colocalization at the cellular level, although close vicinity of expression can be determined (Fig. 2 *C–E*). In juvenile *S. purpuratus*, *pax6* is strongly expressed in the whole area that gives rise to the tube feet (Fig. 2 *F*), thus suggesting that both basal and disk PRCs emerge from a *pax6*-expressing field.

Tube Foot Visual Complex: Cytological Structure and Connection to the Nervous System. Antibody colabeling experiments on tube feet of adult *S. purpuratus* allowed us to further characterize the r-opsin–positive PRCs. Application of anti–acetylated-α-tubulin together with the anti–Sp-Opsin4 antibody showed a large number of cilia surrounding the photoreceptor cells (Fig. 3*A*). Surprisingly, no prominent microvillar structures, as is typical for an r-opsin–expressing PRC type, could be detected using anti–f-actin directed phalloidin staining combined with the anti–Sp-Opsin4 antibody. To clarify the PRC type (microvillar vs. ciliary type) at the ultrastructural level, we first used scanning electron microscopy (SEM) to localize the ciliated cells associated with the PRCs. We found the cells occurring as distinct ciliary patches arranged around the rim of the tube foot disk (Fig. 3*B*). However, by TEM, we found a wide variety of nerve cell types close to the ciliary

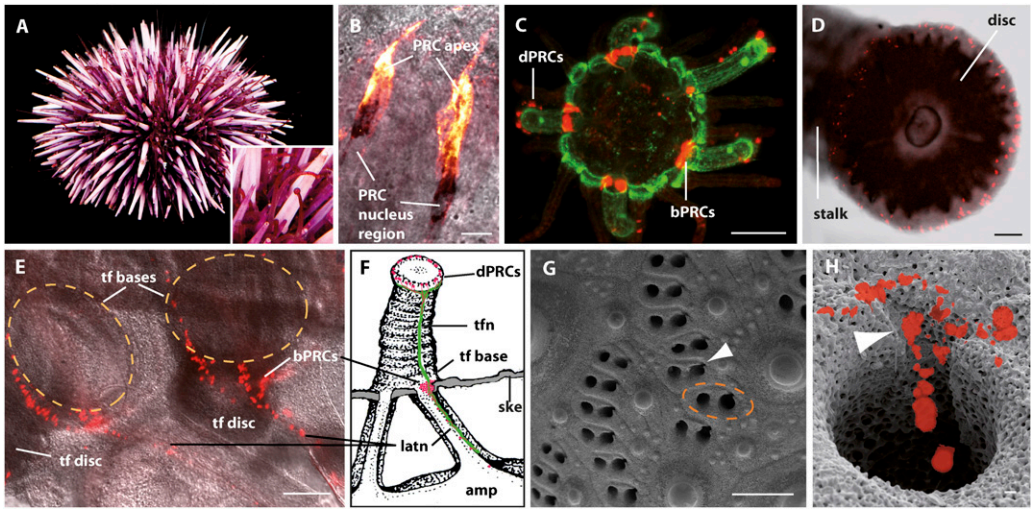

Fig. 1. Tube foot expression of r-opsin in *S. purpuratus*. (*A*) Adult specimen. (*Inset*) Tube feet extended between spines. (*B*) *Sp-opsin4* RNA probe (black) and antibody (yellow) clearly colocalize in disk PRCs (for details, see Fig. S2). (*C*) Sp-Opsin4–positive PRCs (red) at base and disk of primary podia in an early juvenile counterstained with anti-Synaptotagmin B (green), a general echinoderm nervous system marker. (*D*) Disk PRCs arranged around the rim of an adult tube foot disk. Sp-Opsin4 antibody labeling (red). Confocal *z*-stack projected onto confocal laser-scanning microscopic transmission picture. (*E*) Sp-Opsin4 antibody labeling of decalcified adult epidermis reveals PRC clusters at the base of two tube feet. View from former skeletal inside toward external. Note axons and single Sp-Opsin4–positive cells within the lateral nerve (latn) originally leading through tube foot pores (tf, tube foot; orange dotted line: tube foot base where it normally attaches to the skeleton; for details see Fig. S3). (*F*) Schematic drawing (tube foot morphology adapted from Goldschmid) (53) of disk (dPRCs) and basal (bPRCs) PRCs (red) connecting to the nervous system (green) (amp, tube foot ampulla; ske, calcite endoskeleton; tfn, tube foot nerve). (*G*) SEM of adult skeleton. Each tube foot covers one double-pore, one of them bearing an extra channel to accommodate the tube foot lateral nerve (arrowhead) (see also *H* and Fig. 4*C*). Orange dotted line indicates insertion of tube foot in intact animal. (*H*) Illustration depicting Sp-Opsin4–positive PRCs embedded in a depression of the upper tube foot nerve channel. (PRCs clipped out from fluorescent microscope picture of decalcified specimen and projected onto SEM picture of calcite skeleton of another specimen). [Scale bars, 100 μm (*C–E*, and *G*) and 10 μm (*B* and *H*).]

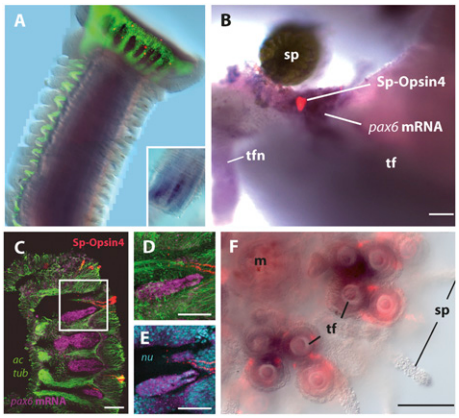

Fig. 2. Tube foot expression of *pax6* in *S. pupuratus*. (*A*) Tube foot whole mount (picture composed of three single photographs). *Sp-pax6* RNA (purple) expressed in the stalk (note insert depicting stalk portion with peeled off epidermis) and Sp-Opsin4–positive PRCs in the disk (red). Nerve fibers stained by anti–acetylated-α-tubulin (green). (*B*) *Sp-pax6*–positive field (purple) and embedded Sp-Opsin4–positive basal PRCs (red); decalcified specimen. (*C–E*) Tube foot disk, lateral view; same staining methods and color depiction as applied in *A* (ac tub, acetylated tubulin). To enhance *Sp-pax6* RNA staining, Cy3-tyramide amplification was used. (*D* and *E*) A magnification of the box in *C*, demonstrating presence of cell nuclei (nu; cyan) in the *Sp-pax6*–positive (purple) region. (*F*) Strong *Sp-pax6* expression (purple) and Sp-Opsin4–positive PRCs (red) in developing tube feet of a juvenile sea urchin (m, mouth; sp, spine; tf, tube foot; tfn, tube foot nerve). [Scale bars, 100 μm (*B* and *F*) and 50 μm (*C–E*).]

patches. Using immunogold detection of Sp-Opsin4 on TEM serial sections allowed us to also determine the r-opsin–positive PRCs using conventional TEM, based on their unusual ultrastructure (Fig. 3 *C–E* and Fig. S4). The PRCs show an apical membrane enlargement bearing many microvilli. A single unmodified cilium (Fig. 3 *D* and *E*), which is often found in microvillar PRCs (20, 21), does not appear to contribute extensively to surface enlargement and, hence, we can clearly classify the Sp-Opsin4–expressing cells as a microvillar PRC type. The PRC cytoplasm makes the cells easily distinguishable from all surrounding nerve cell types by being completely filled with numerous clear vesicles of differing size (Fig. 3*D*). Because we could identify the PRC type as microvillar, it is probable that these vesicles comprise part of an extensive membrane turnover process that is common in microvillar PRCs (22). Surprisingly, detailed TEM observations failed to detect the presence of any kind of screening pigment either in the PRCs themselves or in their vicinity.

All PRCs in the sea urchin tube foot do connect to the nervous system of the animal. Those PRCs in the rim of the tube foot disk send their axons into branches of the tube foot nerve pervading the disk area, and this could be shown using double labeling by anti–Sp-Opsin4 and anti–acetylated-α-tubulin (Fig. 3*F*), as well as by TEM (Fig. S5 *A* and *B*). The PRCs located at the tube foot base project axons through the tube foot pores inside the animal skeleton (Fig. 1 *E* and *H*). A few PRCs are located within the tube foot nerve itself, where it has already entered the internal opaque skeleton (Figs. 1*E* and 3*G*). In early *S. purpuratus* juveniles, double immunolocalization of Sp-Opsin4 and SynaptotagminB (an echinoderm nervous system marker) (23) showed the basal PRCs to project their axons as far as into the developing radial nerves of the animal (Fig. 3*H*). The connection of Sp-Opsin4–positive PRCs to the sea urchin nervous system is displayed in the schemes of Fig. 3 *I* and *J*.

Phototaxis requires the restriction of the angular width over which light can reach the PRCs. As *S. purpuratus* lacks any PRC-associated screening pigment, the animal must have evolved another mechanism to account for that sensory ability.

R-Opsin Expression in a Sea Star Optic Organ. Because of the expression of different opsin genes in *S. purpuratus*, one important target in characterizing the newly discovered r-opsin–positive PRCs was to determine their possible function. Optic cushions of sea stars are, until now, the only optic organs in echinoderms that have been demonstrated to play a part in phototaxis (24). We therefore examined optic cushions of juvenile sea star *Asterias rubens* by coapplying our anti–Sp-Opsin4 antibody and anti-SynaptotagminB. Optic cushions develop in the primary podia of the animal and are thus present from the early juvenile stage on (Fig. 4*A*). Double-

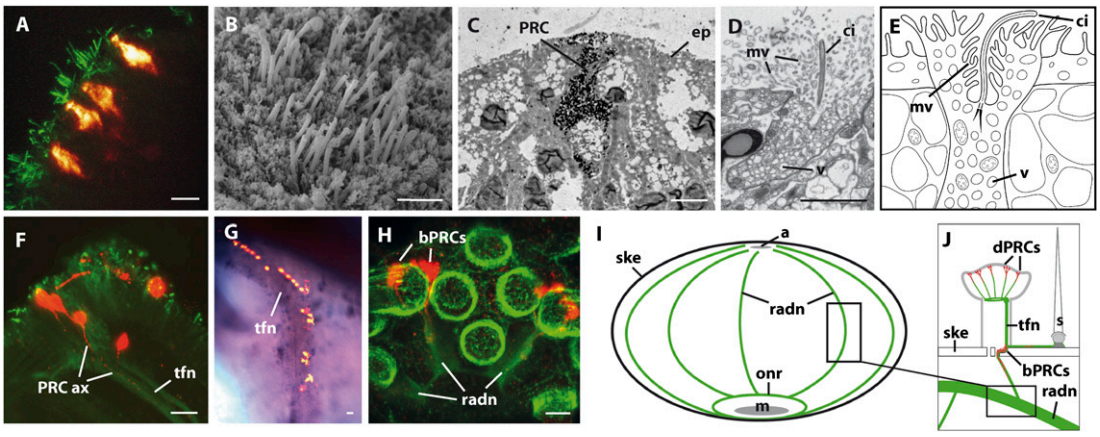

Fig. 3. Tube foot visual complex: cytological structure and connection to the nervous system. (*A*) Sp-Opsin4 immunostaining of sucker PRCs (hot red) close to bundles of cilia (anti–acetylated-α-tubulin immunostaining) (green). (*B*) SEM of ciliary field on tube foot disk epidermis. (*C*) TEM ultrasection showing PRC detected by immunogold labeling against Sp-Opsin4 (ep, epidermis) (for details, see Fig. S4). (*D*) Apical region of PRC bearing numerous microvilli (mv) and a cilium (ci) as well as a huge amount of vesicles (v) (conventional TEM). (*E*) EM-based scheme of tube foot disk PRC. (*F*) Disk Sp-Opsin4–positive PRCs connecting to apical branches of the tube foot nerve (tfn) double localized by anti–Sp-Opsin4 (red) and anti–acetylated-α-tubulin (green) (ax, axon). (*G*) Lateral nerve from decalcified adult epidermis. Anti–Sp-Opsin4 staining (hot red) and *Sp-pax6* mRNA (dark purple). (*H*) *S. purpuratus* juvenile: Sp-Opsin4–positive basal PRCs (red) projecting axons into the developing radial nerves (radn) (green) stained by anti-SynaptotagminB. (*I*) Scheme of the sea urchin internal nervous system (green): the five radial nerves connecting to the oral nerve ring (onr) (a, anus; m, mouth; ske, skeleton). (*J*) Scheme of tube foot and spine innervations (green) and relative position of Sp-Opsin4–positive PRCs (s, spine). [Schemes (*I* and *J*) modified after Burke (10).] [Scale bars, 10 μm (*A*), 2.5 μm (*B–D*), and 25 μm (*F* and *G*).]

labeling experiments show a conspicuous staining of r-opsin protein within the pigmented area of the optic cushion where the somata of the PRCs are located (25), which is accompanied by synaptotagminB-positive nerve cells (Fig. 4*B*). Specific reaction of the Sp-Opsin4 antibody in a sea star optic organ, which is known to have a role in phototaxis, strongly suggests a similar function of this photopigment type in sea urchin too.

Sea Urchin Visual PRC System: A Proposed Model. When not attached to a surface, sea urchin tube feet are highly motile and constantly sway around. Thus, the PRCs in the rim of the tube foot disk will receive light from almost all directions. As they do not possess any screening pigment, a minimum spatial resolution accounting for even simple forms of spatial vision or directed movement can, from our existing data, not be suggested. Nevertheless, these PRCs may be responsible for short-circuit reflex reactions, such as the sharp tube foot withdrawal upon shading reported in *Psammechinus miliaris* (26).

Contrasting with the disk elements, the PRCs at the podial base are not subjected to such intense movements but keep their position close to the animal skeleton. The opaque calcite skeleton of *S .purpuratus* provides shielding to one side of this basal PRC cluster. Depending on the position of the tube foot protruding from an oral, lateral, or aboral part of the skeleton, the skeleton provides a varying shading angle. Our analysis showed that the PRCs are not just located superficially on top of the skeleton, but instead are embedded in a cup-shaped depression of the tube foot pore (Fig. 1 *G* and *H*). We thus used μCT scanning to exactly determine the 3D morphology of the skeletal pore depression. These data provide evidence for a shading angle of up to 272°, corresponding to the measured opening angle of this depression of up to 88° (Fig. 4 *C–E*). By this kind of shielding of the basal PRC clusters, an important optical requirement allowing for directional vision can be fulfilled.

Strong support for the skeleton comprising an essential component of the photoreceptive system in sea urchins comes additionally from our data regarding the onset of phototaxis in juvenile *S. purpuratus* and *P. lividus*. In both species, expression of Sp-Opsin4 protein has been detected as early as in larval rudiment formation. However, despite presence of the photopigment in tube foot disk and basal PRCs, the juveniles do not show phototactic behavior until their skeletogenesis is complete, such that sufficient skeletal plates have formed to build a closed, roundish skeleton (Fig. 4 *F–K*). From this time (around 1 mo in both species in the experimental condition used), the animals show clear negative phototaxis when exposed to full-spectrum artificial light.

Based on our data, we propose the sea urchin visional photoreceptor system to function rather like a huge compound eye. Using the shadow of its own skeleton, the animal is able to detect differences in light intensity relative to its body position. Light input from the basal PRCs conducted and processed via the radial nerves and most probably the oral nerve ring interconnecting them, would then enable the sea urchin to perform directed movement when illuminated from a certain direction.

Discussion

We present a unique integrated study combining molecular, structural, and behavioral data to characterize distinct PRCs in an echinoderm. In negatively phototactic *S. purpuratus*, we found PRCs arranged in clusters at the base of the sea urchin tube feet and in the rim of the tube foot disk. These PRCs express an r-opsin–type photopigment, have a microvillar structure and, at least in the case of the basal cluster, emerge from a *pax6*-positive field. The latter cluster is embedded in a depression in the opaque sea urchin skeleton that shields the PRCs against incoming light with an angle of up to 272°. The basal PRC axons connect to the radial nerves of the developing nervous system. These findings allow us to consider the evolution of form and function of echinoderm PRCs from a completely different perspective from previous studies.

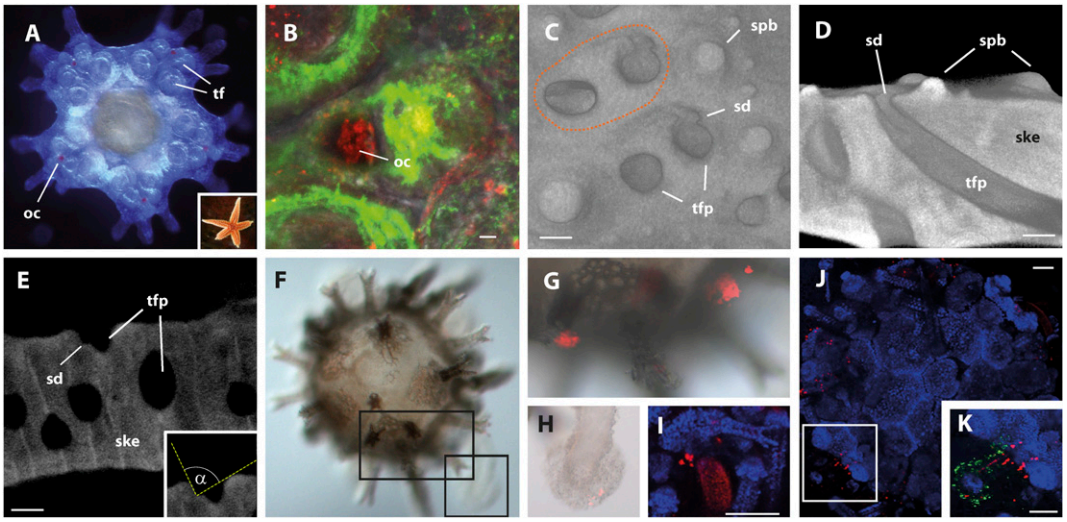

Fig. 4. Visual r-opsin in sea star and phototaxis-related function of the sea urchin skeleton. (*A*) Juvenile *Asterias rubens* with optic cushions (oc) and developing tube feet (tf); (*Inset*) adult specimen. (*B*) R-opsin protein (red) in optic cushion and nerve cells labeled (green) by anti-SynaptotagminB. (*C–E*) 3D-visualized μCT data. (*C*) Volume-rendered 3D model showing two tube feet double-pores of an adult specimen of *S. purpuratus* and depiction of tube foot insertion (orange dotted line). One of the double-pores shows a depression leading inside the tube foot pore (tfp) (sd, skeletal depression; spb, spine base). (*D*) Volume-rendered 3D model showing virtual cross section of the skeleton with tube foot pore leading diagonally through the calcite stereom (ske, skeleton). Note the depression in the apical part of the pore. (*E*) Virtual vertical cross section of a tube foot pore showing the morphology of the skeletal depression and the resulting illumination angle (*Inset*: illumination angle α: 88°). (*F*) Early, nonphototactic, *S. purpuratus* juvenile, at the onset of stereom skeletogenesis. (*G* and *H*) Details from *F* showing basal (*G*) and disk (*H*) Sp-Opsin4–positive PRCs detected by antibody staining (red). (*I*) Developing skeletal elements visualized by reflection confocal laser-scanning microscopy (blue) being exclusively present at primary spine bases. (*J*) One-month-old, phototactic *S. purpuratus* juvenile with complete skeleton. (*K*) Detail from *J* showing basal and disk Sp-Opsin4–positive PRCs (red) in tube foot counterstained with anti–acetylated-α-tubulin (green). [Scale bars, 5 μm (*B*), 300 μm (*D* and *E*), and 100 μm (*I–K*).]

Echinoderm Eyes: Deployment of Canonical Eye Genes and PRC Connection to the Nervous System. *Sp-pax6* and *Sp-opsin4* expression in the purple sea urchin PRCs indicate the presence of a conserved molecular apparatus that serves PRC formation in echinoderms as in many other bilaterian animals (15–18, 27–29). Because *pax6* expression suggests conservation of the specification process of the PRCs and opsin expression is crucial in PRC function, we hypothesize conservation of at least part of an upstream gene regulatory network deploying canonical eye genes in echinoids. This view is supported by findings of Burke et al. (10), who demonstrated tube foot expression for other well-known upstream regulators of eye formation, as well as for genes playing a role in later events of cell type specification and differentiation, such as members of the *six* gene family, *rx*, *atonal*, *neuroD*, and *barh1*. In contrast, the morphological organization of the echinoid PRC system, as well as the arrangement of functional optic organs, differs considerably from that in other metazoans. In sea urchins, not even the simplest "proto-eye" is present in terms of a PRC being partially shielded by pigment and thus allowing for directional vision (15, 30, 31). In addition to the lack of a typical "eye-organ," the echinoid PRC arrangement in regard to the nervous system is also unique among metazoans. Whereas many bilaterian PRCs directly connect to the central nervous system, in sea urchins they project into the tube foot nerve and the radial nerves. As physiological studies showed that ring and radial nerves are essential for phototaxis in sea stars and sea urchins (1, 32, 33), it can thus be concluded that, although the tube foot nerve has to be considered a more peripheral part of the echinoid nervous system, the basal tube foot PRCs connecting to the radial nerves might very well serve a functional "central nervous system" with inputs on photoreception.

Different Compound Eye Models in Echinoderms. In the past, although lacking any structural evidence for distinct PRCs, different authors have suggested a compound eye model for echinoderm vision. Woodley (34), studying photobehavior of the tropical sea urchin *Diadema antillarum*, first suggested that the entire animal functions as a compound eye, with the spines screening off-axis light. Similarly, Blevins and Johnsen (13) introduced their model for two different echinoid species of the genus *Echinometra*, which they showed to possess a certain degree of spatial vision. Subsequent work on *S. purpuratus* (3) again indicated spatial vision with an even higher optical resolution than in *Echinometra*. Both studies were based on the assumption that, according to the long hypothesized "diffuse" dermal-light sense in echinoderms (2, 8, 9), the whole body surface of the sea urchins would be photosensitive. The spatial resolution of the PRC system would then depend on the spacing of spines that function, similarly to pigment cells in insect ommatidia, by shading defined parts of the sea urchin's skin. In contrast, our findings of distinct PRCs contradict the prerequisite of the model proposed by Johnsen and colleagues (3, 13) and are supported by the findings of Millott and Coleman (35), who demonstrated that the podial bases in sea urchins comprise the most photosensitive part of their skin. Our finding that the basal PRC cluster is embedded in a considerable depression of the tube foot pore, resulting in a smaller angular width of the light reaching the PRCs (Fig. 4*E*), may constitute one component of a detector system accounting for the behavioral results presented by Johnsen and associates (3, 13). Nevertheless, a new model implementing our structural findings and additional parameters like (species-dependent) number and arrangement of tube feet will have to show if and how different spacing of spines relative to the discovered tube foot basal PRCs might influence spatial resolution of the echinoid PRC system.

The second proposed compound eye model referred to the photoreceptor system of a brittle star (12). The authors demonstrated the arms of the light-sensitive species *Ophiocoma wendtii* to possess specialized calcite skeletal structures that possibly function as microlenses in guiding and focusing the light inside the deeper tissues of the animal. The PRCs deployed in that scenario remained unknown except for their assumed position within a bundle of nerve cells underlying the arm ossicles in the focal plane of the microlenses. The actual compound eye would then comprise a huge array of such lens- and photosensitive nerve cell units within the animal's arms.

Comparing our results on *S. purpuratus* with the model proposed for brittle stars, one interesting similarity emerges: the use of calcite skeletal material to form part of a photoreceptive system. However, although we propose the sea urchins' opaque calcite stereom to comprise a shielding device for each PRC cluster, resulting in numerous compound eye units, brittle stars are thought to use a different mechanism by focusing light through transparent calcite crystal elements onto light-sensitive nerve bundles. As nothing is yet known about the deployed PRC type and organization in brittle stars, we can only speculate about possible similarities to the sea urchin PRC system. Nevertheless, it is noteworthy to point out that sea urchins, sea stars, and brittle stars deploy highly divergent functional units to achieve vision and thus comprise another surprising example of evolution driving optic organ diversification in relatively closely related animals by rearranging a given set of (cellular) components.

The association of the characterized PRC type with podia seems to be a more general phenomenon in echinoderms. The starfish optic cushions lie at the base of the terminal tentacles, which arise from the first developing, primary podia (36, 37). Homology of the respective PRCs to the sea urchin PRCs is evidenced by a similar microvillar design (25) and the positive immunoreactivity to the anti–Sp-Opsin4 antibody. Likewise, the microvillar PRCs of synaptid sea cucumber eyes reside in the feeding tentacles arising from the first developing podia (38). The presence of pigmented supporting cells in sea stars as well as in sea cucumbers reflects the standard design of simple pigmented eyes and may represent the ancestral condition. Pigmentation is therefore most likely lost secondarily in sea urchins and shading of the PRCs is taken over by the underlying skeletal elements.

r-Opsin–Expressing PRC Serving Vision in a Deuterostome Animal. Compared with r-opsin–positive PRCs of protostome animals, which usually form part of cerebral eyes, the sea urchin tube foot PRCs stand out by their patchy distribution across the body. In the case of echinoderms, anatomical data are, however, of limited value for evolutionary considerations. Morphological data hitherto failed to uncover which parts of the adult echinoderm nervous system correspond to the central nervous system and especially to the brain of other animals. Conversely, molecular data are just emerging that allow for comparison within metazoans (10). Given the expression of genes involved in patterning vertebrate retinal development in sea urchin tube feet (10) and our findings of tube foot PRCs forming within an expression domain of *pax6*, we can now propose that the uncovered PRCs are evolutionary linked to r-opsin–positive eye PRCs of other animals.

The former view that microvillar PRCs are exclusively present in protostome eyes (20, 39) has been overtaken by molecular photoreceptor research (27). Although vertebrates have been lately shown to possess r-opsin–expressing PRCs in their retina (40–44), deuterostome animals have been generally thought to deploy ciliary type PRCs for vision (39). Vertebrate r-opsin–expressing PRCs have long been morphologically overlooked because of their lack of any specialized membrane enlargement, and they are clearly not used for vision. Instead, these PRCs mediate the pupillar reflex and entrain the circadian clock. The few known examples of deuterostome animals possessing microvillar PRCs comprise a tornaria larva of an enteropneust (45, 46), the lancelet Joseph cells and Hesse eyecups (47–50), a tunicate salp (51), and sea stars with their optic cushions (27, 52). With the single exception of sea star optic cushions, none of the other microvillar PRCs has been shown to serve vision. This finding leads unavoidably to the question of when, during evolution, the functional shift between microvillar PRCs serving vision (as in proto-

stomes and sea stars) and their nonvisual function in vertebrates might have taken place.

Our data provide evidence of microvillar, r-opsin–expressing PRCs acting as visual receptors in a deuterostome, nonvertebrate animal. We thus propose that the visual function of the r-opsin–positive type of PRCs has to be considered ancestral not only for protostomes, but also for deuterostomes and the bilaterian ancestor. Because of similar gene regulatory networks in protostome and vertebrate eye development, this type of PRC most probably already formed part of a cerebral eye system in their last common ancestor. In deuterostomes, visual function was maintained in the lineage leading to echinoderms but, at least in sea urchins, the cells were considerably reorganized and a unique compound-eye–like mode of data processing emerged. In the lineage leading to vertebrates, the PRCs kept their position in cerebral eyes, but now became involved in circadian rhythms. According to our data, this dramatic functional shift occurred no earlier than during the emergence of chordates.

Materials and Methods

Descriptions of animal supply and culture and phototaxis experiments, can be found in *SI Materials and Methods*. Technical information regarding antibody production and purification, SEM and TEM, and X-ray microtomography (μCT) also included in this section. Additionally, references for detailed protocols regarding in situ hybridization, immunohistochemistry, and immunogold labeling for TEM are contained in *SI Materials and Methods*.

ACKNOWLEDGMENTS. We thank P. Leahy and the Southern California Sea Urchin Company for constant supply of *S. purpuratus* adults and juveniles; R. Burke for kindly providing the anti-SynaptotagminB antibody; A. Cameron, for critical discussion; E. Davidson and M. Thorndyke for helpful comments on the manuscript; M. Ormestad/KahiKai for providing the photograph of *S. purpuratus* in Fig. 1*A*, and G. Benvenuto for support with confocal microscopy; D. Lovera for tirelessly raising sea urchin larvae and juveniles and for assistance in phototaxis experiments; and J. Müller for access to the μCT scanner and A. Ziegler for assistence with μCT scanning and 3D visualization. This work was supported in part by German Research Foundation (Deutsche Forschungsgemeinschaft) Grant HA 4443/4-1 and by Marie Curie Research Training Network Zoonet Fellowship MRTN-CT-2004-005624 (to E.A.).

1. Yoshida M (1966) Photosensitivity. *Physiology of Echinodermata*, ed Boolootian RA (John Wiley and Sons, New York), pp 435–464.
2. Millott N (1975) The photosensitivity of Echinoids. *Adv Mar Biol* 13:1–52.
3. Yerramilli D, Johnsen S (2010) Spatial vision in the purple sea urchin *Strongylocentrotus purpuratus* (Echinoidea). *J Exp Biol* 213:249–255.
4. Sarasin CF, Sarasin PB (1887) Eyes and integument of the *Diadematids* (Translated from German) In *Ergebnisse naturwissenschaflicher Forschung auf Ceylon* (CW Kreidel's Verlag, Wiesbaden, Germany).
5. Millott N (1953) Light emission and light perception in species of *Diadema*. *Nature* 171:973–974.
6. Millott N (1954) Sensitivity to light and the reactions to changes in light intensity of the echinoid, *Diadema antillarum* Philippi. *Philos T Roy Soc B* 238:187–220.
7. Millott N, Manly BM (1961) The iridiophores of the echinoid *Diadema antillarum*. *Q J Microsc Sci* 102:181–194.
8. Hyman LH (1955) Echinodermata. *The Invertebrates*, ed Boell EJ (Mc-Graw-Hill, New York), Vol 4.
9. Yoshida M, Takasu N, Tamotsu S (1984) Photoreception in echinoderms. *Photoreception and Vision in Invertebrates*, ed Ali MA (Plenum Press, New York), pp 743–772.
10. Burke RD, et al. (2006) A genomic view of the sea urchin nervous system. *Dev Biol* 300: 434–460.
11. Raible F, et al. (2006) Opsins and clusters of sensory G-protein-coupled receptors in the sea urchin genome. *Dev Biol* 300:461–475.
12. Aizenberg J, Tkachenko A, Weiner S, Addadi L, Hendler G (2001) Calcitic microlenses as part of the photoreceptor system in brittlestars. *Nature* 412:819–822.
13. Blevins E, Johnsen S (2004) Spatial vision in the echinoid genus *Echinometra*. *J Exp Biol* 207:4249–4253.
14. Giese AC, Farmanfarmaian A (1963) Resistance of the purple sea urchin to osmotic stress. *Biol Bull* 124:182–192.
15. Gehring WJ, Ikeo K (1999) *Pax 6*: Mastering eye morphogenesis and eye evolution. *Trends Genet* 15:371–377.
16. Gehring WJ (2002) The genetic control of eye development and its implications for the evolution of the various eye-types. *Int J Dev Biol* 46:65–73.
17. Pichaud F, Desplan C (2002) *Pax* genes and eye organogenesis. *Curr Opin Genet Dev* 12:430–434.
18. Fernald RD (2006) Casting a genetic light on the evolution of eyes. *Science* 313: 1914–1918.
19. Czerny T, Busslinger M (1995) DNA-binding and transactivation properties of *Pax-6*: Three amino acids in the paired domain are responsible for the different sequence recognition of Pax-6 and BSAP (Pax-5). *Mol Cell Biol* 15:2858–2871.
20. Eakin RM (1979) Evolutionary significance of photoreceptors: In retrospect. *Am Zool* 19:647–653.
21. Purschke G, Arendt D, Hausen H, Müller MCM (2006) Photoreceptor cells and eyes in Annelida. *Arthropod Struct Dev* 35:211–230.
22. Blest AD (1988) The turnover of phototransductive membrane in compound eyes and ocelli. *Advanced Insect Physiology* 20:1–54.
23. Burke RD, et al. (2006) Neuron-specific expression of a synaptotagmin gene in the sea urchin *Strongylocentrotus purpuratus*. *J Comp Neurol* 496:244–251.
24. Yoshida M, Ohtsuki H (1968) The phototactic behaviour of the starfish *Asterias amurensis* Lütken. *Biol Bull* 134:516–532.
25. Penn PE, Alexander CG (1980) Fine structure of the optic cushion in the asteroid *Nepanthia belcheri*. *Mar Biol* 58:251–256.
26. Millott M, Yoshida M (1956) Reactions to shading in the sea urchin *Psammechinus miliaris* (Gmelin). *Nature* 178:1300.
27. Arendt D (2003) Evolution of eyes and photoreceptor cell types. *Int J Dev Biol* 47: 563–571.
28. Arendt D, Tessmar-Raible K, Snyman H, Dorresteijn AW, Wittbrodt J (2004) Ciliary photoreceptors with a vertebrate-type opsin in an invertebrate brain. *Science* 306: 869–871.
29. Vopalensky P, Kozmik Z (2009) Eye evolution: Common use and independent recruitment of genetic components. *Philos Trans R Soc Lond B Biol Sci* 364:2819–2832.
30. Arendt D, Wittbrodt J (2001) Reconstructing the eyes of Urbilateria. *Philos Trans R Soc Lond B Biol Sci* 356:1545–1563.
31. Land MF, Nilsson DE (2002) *Animal Eyes*, ed Willmer P and Norman D (Oxford University Press, London).
32. Holmes SJ (1912) Phototaxis in the sea urchin *Arbacia*. *J Anim Behav* 2:126–136.
33. Yoshida M, Ohtsuki H (1966) Compound ocellus of a starfish: Its function. *Science* 153: 197–198.
34. Woodley JD (1982) Photosensitivity in *Diadema antillarum*: Does it show scototaxis? In *The International Echinoderm Conference, Tampa Bay* September 14–17, 1981, ed Lawrence JM (AA Balkema, Rotterdam), p 61.
35. Millott N, Coleman R (1969) The podial pit—A new structure in the echinoid *Diadema antillarum* Philippi. *Z Zellforsch Mikrosk Anat* 95:187–197.
36. Morris VB, Selvakumaraswamy P, Whan R, Byrne M (2009) Development of the five primary podia from the coeloms of a sea star larva: Homology with the echinoid echinoderms and other deuterostomes. *Proc Biol Sci* 276:1277–1284.
37. Atwood DG (1973) Larval development in the asteroid *Echinaster echinophorus*. *Biol Bull* 144:1–11.
38. Yamamoto M, Yoshida M (1978) Fine structure of the ocelli of a synaptid holothurian, *Opheodesoma spectabilis*, and the effects of light and darkness. *Zoomorphology* 90: 1–17.
39. Eakin RM (1982) Continuity and diversity in photoreceptors. *Visual Cells in Evolution*, ed Westfall J (Raven Press, New York), pp 91–105.
40. Provencio I, et al. (2000) A novel human opsin in the inner retina. *J Neurosci* 20: 600–605.
41. Hattar S, Liao HW, Takao M, Berson DM, Yau KW (2002) Melanopsin-containing retinal ganglion cells: Architecture, projections, and intrinsic photosensitivity. *Science* 295:1065–1070.
42. Rollag MD, Berson DM, Provencio I (2003) Melanopsin, ganglion-cell photoreceptors, and mammalian photoentrainment. *J Biol Rhythms* 18:227–234.
43. Fu Y, Liao HW, Do MT, Yau KW (2005) Non-image-forming ocular photoreception in vertebrates. *Curr Opin Neurobiol* 15:415–422.
44. Bellingham J, et al. (2006) Evolution of melanopsin photoreceptors: Discovery and characterization of a new melanopsin in nonmammalian vertebrates. *PLoS Biol* 4:e254.
45. Brandenburger JL, Woollacott RM, Eakin RM (1973) Fine structure of eyespots in tornarian larvae (phylum: Hemichordata). *Z Zellforsch Mikrosk Anat* 142:89–102.
46. Nezlin LP, Yushin VV (2003) Structure of the nervous system in the tornaria larva of *Balanoglossus proterogonius* (Hemichordata: Enteropneusta) and its phylogenetic implications. *Zoomorphology* 123:1–13.
47. Lacalli TC (2004) Sensory systems in amphioxus: A window on the ancestral chordate condition. *Brain Behav Evol* 64:148–162.
48. Koyanagi M, Kubokawa K, Tsukamoto H, Shichida Y, Terakita A (2005) Cephalochordate melanopsin: Evolutionary linkage between invertebrate visual cells and vertebrate photosensitive retinal ganglion cells. *Curr Biol* 15:1065–1069.
49. Nasi E, del Pilar Gomez M (2009) Melanopsin-mediated light-sensing in amphioxus: A glimpse of the microvillar photoreceptor lineage within the deuterostomia. *Commun Integr Biol* 2:441–443.
50. Gomez MdelP, Angueyra JM, Nasi E (2009) Light-transduction in melanopsin-expressing photoreceptors of Amphioxus. *Proc Natl Acad Sci USA* 106:9081–9086.
51. Gorman ALF, McReynolds JS, Barnes SN (1971) Photoreceptors in primitive chordates: Fine structure, hyperpolarizing receptor potentials, and evolution. *Science* 172: 1052–1054.
52. Eakin RM, Brandenburger JL (1979) Effects of light on ocelli of seastars. *Zoomorphology* 92:191–200.
53. Goldschmid A (2007) In *Spezielle Zoologie, Bd.1 Einzeller und Wirbellose Tiere [Special Zoology, Vol. 1 Unicellular and Invertebrate Animals]*, eds Westheide W, Rieger R (Spektrum Akademischer Verlag, Heidelberg).